ISSN 1392–1320 MATERIALS SCIENCE (MEDŽIAGOTYRA). Vol. 25, No. 4. 2019

# Effect of Er Addition on the High Temperature Strength of Al-Si-Cu-Ni-Mg-Fe Piston Alloys by T5 and T6 Heat Treatment

**Xianfeng LI, Cunjuan XIA, Yi WU, Dong CHEN, Mingliang WANG *, Naiheng MA, Haowei WANG**

*School of Materials Science & Engineering, Shanghai Jiao Tong University, No. 800 Dongchuan Road, Shanghai 200240, P. R. China*

crossref http://dx.doi.org/10.5755/j01.ms.25.4.19453

*Received 10 November 2017; accepted 10 June 2018*

In this study, the dependence of Er addition (0 – 0.49 wt.%) on the microstructural evolution and related tensile strength at high temperature (HT) were investigated for the eutectic Al-Si piston alloys. The results showed there were intermetallic compounds of γ-$Al_3CuNi$, δ-$Al_7Cu_4Ni$, $Al_4Cu_2Mg_8Si_7$, β-AlFeSi and $Al_3$(Er, Cu, Fe)(Ni, $Si)_2$ identified at T5 states. Herein, the added Er element has led to the formation of the star-like and the irregular-shaped $Al_3$(Er, Cu, Fe)(Ni, $Si)_2$ phase. The phase was stable which showed little change in both size and composition experienced solid solution at HT during the T6 treatment. For the HT strengths (350 °C), the T5 state alloys have higher UTSs than those at T6 state, both of which were reduced gradually with the increasing Er contents. The variation of HT strengths caused by the Er addition was explained by the microstructral evolution, namely $Al_3$(Er, Cu, Fe) (Ni, $Si)_2$ phase formation
*Keywords:* eutectic Al-Si alloy, tensile strength, rare earth element, heat treatment.

## 1. INTRODUCTION

In automotive, transportation and general engineering fields, the Al-Si alloys are widely applied to reduce component weight to improve the fuel economy [1 – 6]. Such alloys are of great commercial importance due to their high fluidity and low shrinkage characteristics in the casting, brazing and welding processes [1]. Furthermore, the high hardness of both eutectic and primary Si particles has rendered the outstanding wear resistance to these alloys. Nevertheless, all these Si phases often exhibit facet edges, which is detrimental to the mechanical properties of Al-Si alloys because these sharp tips and edges may act as the stress concentrators under forces [7, 8].

To solve this problem, many works have been performed to refine and modify the primary and eutectic Si structure of Al-Si alloys. Numerous techniques are used to refine or modified the size and morphology of Si structure, including chemical modification using modifiers [9] or nucleation agents [10], melt super-heating treatment [11], rapid solidification [12], spray forming [13] and outfield treatment [14]. From the perspective of industrial application, the utilization of chemical modifiers into Al-Si alloys is one of the most practical methods owing to its effectiveness and simplicity. In the literatures, many investigations have been performed to examine the influences of rare earth elements on the Si morphology and size, and related effects on the mechanical properties in Al-Si alloys, i.e., Ce [15, 16], Eu [17], Er [18 – 23], La [24, 25], Sc [26, 27], Y [28] and Yb [29]. For example, Han et al. [18] studied the effect of Er on eutectic Si and tensile strengths at room temperature (RT) of Al-8Si alloy. They found that the coarse flake-like eutectic Si was modified to refined plate-like structure, and the tensile strength at RT was improved accordingly with the addition of Er from 0 to 0.5 wt.%. Hu et al. [21] found that Er can effectively refine the coarse plate-like eutectic Si to a circular structure and to a fine branched and fibrous structure in Al-11.88Si-1.75Cu-0.93Fe alloy gradually. At the same time, the RT ultimate tensile strength (UTS) was increased by 32 % with the 0.6 wt.% Er addition. Li et al. [22] demonstrated both primary and eutectic Si can be refined or modified with the 0.5 wt.% Er addition, in which the UTS at RT was improved by ~75 % in the alloys. Generally, it is found that Er has the effect on the refinement of primary Si [20, 22] and modification of eutectic Si [18, 19, 21, 23], which can thus improve the RT mechanical properties in Al-Si alloys. However, there are few reports discussing the dependence of the Er content on the micro-structural evolution and strength at high temperature (HT) of Al-Si alloys to the best of our knowledge.

The multicomponent Al-Si-Cu-Ni-Mg-Fe alloys, inside the range of the eutectic Al-Si alloys, are the main choice of piston material in automotive industries [30 – 32]. Since the service conditions for pistons are very tough and complicated, the Al-Si alloys are required to withstand longtime service at temperatures from 350 to 400 °C [33]. Therefore, the super HT strength is critical design of piston alloy. To elevate the HT strength of Al-Si alloy, the introduction of heat-resistant intermetallic compounds is a viable strategy. Therefore, many metallic elements are incorporate to create the stable HT compounds to meet demand. Ni is the most selected element in Al-Si alloys [34, 35], since the formation of AlCuNi phase is effective to strengthen the alloys at HT strength. Li et al. [34] reported the introduction of Ni to form $Al_3CuNi$ and $Al_7Cu_4Ni$ in Al-13Si alloy, and thereby elevated the HT strength (350 °C) from 42.74 MPa to 61.63 MPa. Other metal elements can also be added [36 – 39]. For example, Sui et al. [36] studied the micro-structure and mechanical properties of cast Al-12Si-4Cu-

* Corresponding author. Tel.: +86-21-54747597; fax: +86-21-54747597.
E-mail address: *mingliang_wang@sjtu.edu.cn* (M. Wang)

2Ni-0.8Mg alloys with Gd addition. They found the $Al_3CuGd$ phase formed and the morphology of Gd-containing phase gradually developed into needle-like form, and the HT tensile strength (350 °C) were increasing from 69.9 MPa to 76.1 MPa with the 0.2 wt.% Gd addition. Gao et al. [37] added 2 wt.% Zr into Al-13.5Si-3.8Cu-2Ni-1Mg-0.5Fe alloy, and found the HT tensile strength (350 °C) was increased by 15.82 % with the formation of ZrAlSi block-like particles.

Since the Er element has the modifying effect on the Si phases and the positive effect on the RT strength of Al-Si alloys, the dependence of Er addition on the micro-structural evolution and mechanical properties at HT (350 °C) of the multicomponent Al-Si-Cu-Ni-Mg-Fe piston alloys at both T5 and T6 states are studied, and the modification effect and the HT strengthening mechanism are discussed.

## 2. EXPERIMENTAL PART

To prepare Al-Si-Cu-Ni-Mg-Fe-(Er) piston alloys, the available master metals and alloys were utilized, including pure Al (> 99.999 at %) and Mg (> 99.9 at %) ingots, Al – 20 wt.% Si, Al – 50 wt.% Cu, Al – 10 wt.% Ni, Al – 20 wt% Fe and Al – 11 wt.% Er. Al – 11 wt.% Er binary alloy are provided by Huhan Rare Earth Metal Material Research Institute, and the other metals and alloys are purchased from Sichuan Lande High-Tech Industry Company. Firstly, the metals and alloys were melted. Once the melt temperature arrived at 760 °C, the $C_2Cl_6$ was used to cover the melt for 30 minutes to refine the melt, and then removed surface dregs. Secondly, the alloy melts were poured into a permanent mould, which was kept in the 200 °C in advance. Finally, the as-cast ingots were achieved as the mould cooled down.

A series amounts of Er (0, 0.24 and 0.49 wt.%) were added to the base alloys, and the alloys were labeled as alloys 1#, 2# and 3# accordingly (Table 1). The heat treatments of T5 and T6 processes have been performed on the studied alloys. In detail, the as-cast alloys were aged at 200 °C for 8 h (DHG-9140A Electric blower drying oven, Yiheng Scientific Instrumental Company, China) to fulfil the T5 treatment. Regarding T6 state, the as-cast alloys were solution treated for 3 h at 480 °C (N30/65HA resistance furnace, Nabertherm Gmbh, Germany). Following by the cold water quench, the alloys were aged at 200 °C for 8 h, and cooled in the air.

**Table 1.** Chemical compositions of eutectic Al-Si alloys

| Chemical compositions | Element, wt.% | | | | | | |
|---|---|---|---|---|---|---|---|
| | Si | Cu | Mg | Ni | Fe | Er | Al |
| 1# | 13.5 | 5.0 | 0.84 | 2.0 | 0.5 | – | Bal. |
| 2# | 13.5 | 5.0 | 0.84 | 2.0 | 0.5 | 0.24 | Bal. |
| 3# | 13.5 | 5.0 | 0.84 | 2.0 | 0.5 | 0.49 | Bal. |

In the HT tensile tests, the test bars were machined to the "dog-bone" type specimens initially (Fig. 1), and tested universal testing facility (Shimadzu-100KN-A, Shimadzu Corp., Japan). Before the tensile test, the specimen was kept at 350 °C for 30 min. The tests were performed at 1 mm/min. Using a X-Ray diffractometer (D8 ADVANCE XRD, Bruker Corp., Germany) with Cu *K*α radiation (λ = 0.1542 nm), the XRD spectra are achieved to identify the phase compositions of alloys. For the morphological observation, the optical microscope (OM) was used for overall observation at lower magnification. A NOVA Nano SEM 230 Scanning Electron Microscope (SEM) equipped with an energy dispersive X-ray spectroscopy (EDS) was used for local observation and chemical composition analysis at higher magnification. The size of primary Si was analyzed by Nano measurer software.

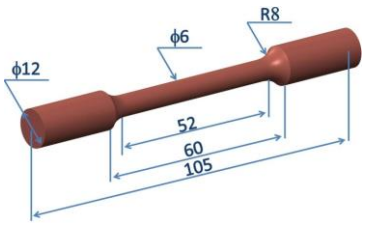


**Fig. 1.** The dimensions for 'dog-bone' type specimens (The unit for the specimen is mm)

## 3. RESULTS AND DISCUSSION

Fig. 2 shows XRD spectra of both T5 and T6 heat treated Al-Si alloys. The main phases of the alloys Al (JCPDS: 89-4037) and Si (JCPDS: 27-1402). Furthermore, the typical intermetallic compounds in the alloys include γ-$Al_3CuNi$ (JCPDS: 65-3454), δ-$Al_7Cu_4Ni$ (JCPDS: 28-0016), $Al_4Cu_2Mg_8Si_7$ (JCPDS: 41-1068), β-AlFeSi (JCPDS: 87-0330) and $Al_3ErNi_2$ (JCPDS: 50-1220).

In XRD spectra, γ-$Al_3CuNi$, δ-$Al_7Cu_4Ni$, β-AlFeSi and $Al_4Cu_2Mg_8Si_7$ phases are found in all T5 state (Fig. 2 a) and T6 state (Fig. 2 b) alloys independent of the Er addition. All these phases are the typical compounds in the Al-Si-Cu-Ni-Mg-Fe piston alloys, as identified in the references [40, 41]. With the addition of Er, the $Al_3ErNi_2$ compound forms in 2# and 3# samples at T5 state (Fig. 2 a). This compound has stably existed in the alloys which have experienced the T6 heat treatment (Fig. 2 b). $Al_3ErNi_2$ can be written in the stoichiometry format of $Al_3(Er, Cu, Fe)(Ni, Si)_2$, which should be characterized in detail in the following sections. $Al_3ErNi_2$ is not reported in the former works about the adding Er element into the Al-Si alloys, while $Al_3Er$ is typically mentioned in the references [21]. For example, Hu et al. [21] investigated the addition of Er into the die-cast Al-11.88Si-1.75Cu-0.93Fe alloy. They claimed the formation of $Al_3Er$ in their alloy, although there was not any direct evidence in their work. Shi et al. [23] added Er element into Al-7.1Si-0.45Mg-0.12Fe alloy, and found the Si, Mg and Fe atoms dissolved in the $Al_3Er$ phases characterized by the EDS analysis.

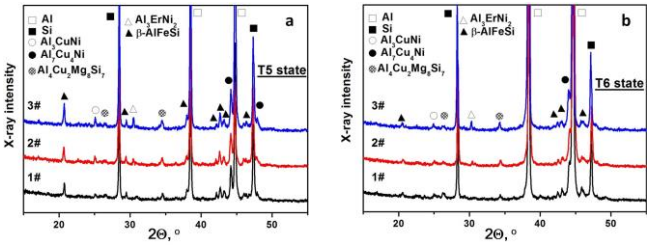


**Fig. 2.** XRD spectra of Al-Si alloys with various addition of Er at both: a – T5; b – T6 states

Therefore, it is proposed that the Al-Er compound has the ability to solutionize the solute atoms in the complex Al-Si alloys.

The optical micrographs of the Al-Si alloys with various Er additions at T5 state are exhibited in Fig. 3 a – c. The typical phases, like eutectic Si, primary Si, needle-like β-AlFeSi, skeleton-like δ-$Al_7Cu_4Ni$ are observed in these alloys. Furthermore, with the addition of Er, some star-like or irregular-shaped compounds are observed in Fig. 3 b and c. These compounds are in the size of 10 ~ 20 μm. Fig. 4 exhibits the element mapping analysis of 3# specimen at T5 state. It is notably found the Er element has mostly aggregated with other alloy elements of Al, Si, Ni, Cu and Fe in either the star-like or irregular-shaped blocks, as labled in Fig. 4. The EDS analyses on the star-like phase (Point 1) and the irregular-shaped blocks (Point 2) show that the compounds have the nearly identical chemical compositions, and can be generalized to the formula $Al_3(Er,Cu,Fe)(Ni, Si)_2$ (Table 2). This is in good compliance with the conclusion drawn from the XRD analysis.

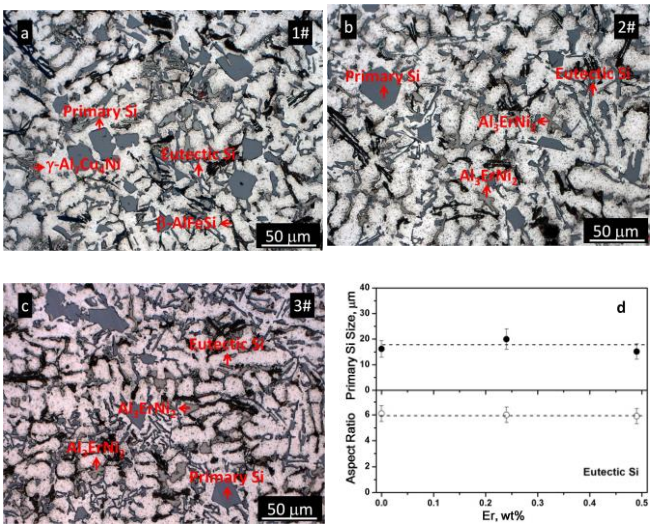


**Fig. 3.** The optical images of various additions of Er: a – 0 % Er; b – 0.24 % Er; c – 0.49 % Er in Al-Si alloys; d – the dependent of primary Si size and aspect ratio of eutectic Si on the Er additions at T5 state

Regarding the eutectic Si particles, they typically have the long strip morphology. The size of eutectic Si phase is quite scattering, where the strip lengths are from 10 to 30 μm. Furthermore, the aspect ratios are ~ 6 irrespective of the Er content (Fig. 3 d). This means the addition of Er have little influence on the morphology of eutectic Si, which is on the contrary with most reported results. For example, Han et al. [18] found the eutectic Si was modified from a coarse flake-like morphology to refined plate-like structure morphology in the Al-8Si alloy with the addition of 0.3 ~ 0.8 wt.% Er. Xing et al. [19] modified Al – 12.6Si alloy using 0.05 ~ 1 wt.% Er. They found the micro-structure of eutectic Si transferred into the fine fiber shape from coarse circular shape, and the size of the eutectic Si was significantly decreased. Notably, the Al-Si alloys used in these works [18, 19] did not contain any alloying element, so that the modifying effect of Er on the eutectic Si can be implemented without any interruption. In the more complex cases, Shi et al. [23] added Er element into Al-7.1Si-0.45Mg-0.12Fe, and found that additions of Er refined the eutectic Si phases in the as-cast state. Hu et al. [21] reported Er modified the eutectic Si in the Al-11.88Si-1.75Cu-0.93Fe. Generally, two alloying elements were included in each of the Al-Si alloy where Er can still realize its modification effect on the eutectic Si. However, there are four alloying elements (i.e., Cu, Ni, Mg and Fe) existing in the Al-Si piston alloys of this work, the Er element is largely consumed to form the $Al_3(Er,Cu,Fe)(Ni, Si)_2$ phase. Therefore, the modification of eutectic Si by Er has not been achieved in this Al-Si alloy. The case of failed modification on the eutectic Si in the multicomponent Al-Si alloys can be found in former works. For instance, Tsai et al. [42] found the >1 wt% Ce addition into Al-7Si-0.35Mg did not modify the eutectic Si morphology because of forming the Ce-23Al-22Si and Al-17Ce-12Ti-2Si-2Mg intermetallics.

The primary Si has generally exhibited the polygonal block morphology. The size of primary Si is in the range of 15 ~ 25 μm, of which the average sizes are measured to be ~ 18 μm independent on the Er addition, as shown in Fig. 3 d. These primary Si sizes have shown the well consistency with the reported data [34, 40, 43] of eutectic Al-Si alloys. This finding has also proved that the Er was almost used to form the $Al_3(Er,Cu,Fe)(Ni, Si)_2$ phase, and thus did not show the refining effect on the primary Si which was suggested in both Xing`s [20] and Li`s [22] works.

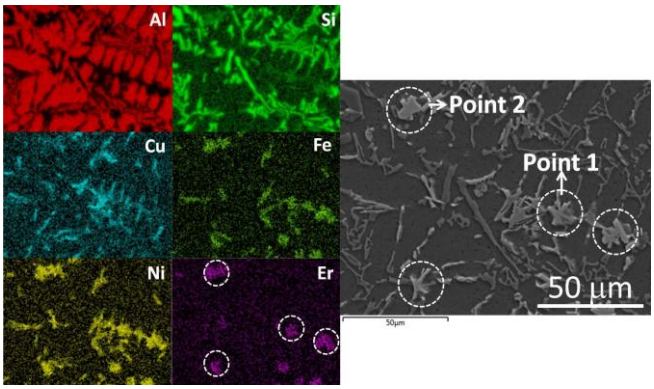


**Fig. 4.** Element mapping analysis of 0.49 wt.% Er added Al-Si alloy at T5 state

Fig. 5 a – c exhibits the optical images of T6 treated eutectic Al-Si alloys with various Er contents. For the primary Si, it has exhibited in the form of block morphology, and the size range is about 10 ~ 25 μm independent on the Er addition (Fig. 5 a – c), which is similar with those primary Si particles at T5 state.

However, the eutectic Si phase has strip morphology which is shorter in length (5 ~ 20 μm) than those at T5 state. Fig. 5 d shows that the aspect ratios of the eutectic Si are ~ 4 regardless of Er content at T6 state. It is seen that the aspect ratio of eutectic Si has been reduced at T6 state, since a high temperature solution treatment can makes spheroidize eutectic Si strips. Such process is called thermal modification. The solution treatment approaching to the temperature of eutectic point is able to intensively alter the morphologies of Si particles [44]. Ogris et al. [45] theoretically studied the spheroidization process of eutectic

Si in Al-Si alloys. It was suggested that spheroidization can occur at temperature as low as 400 ºC, and be well completed within minutes of exposure to temperature > 500 °C. Experimentally, Sebaie et al. [46] observed that during solution treatment at 495 °C and 540 °C, the eutectic Si strip has experienced the shape perturbations, including the fragmentation into small segments, and then spheroidization in Al-Si alloys. Gutiérrez et al. [47] reported the similar spheroidizing process in the eutectic Si phase during solution treatment at 480 °C.

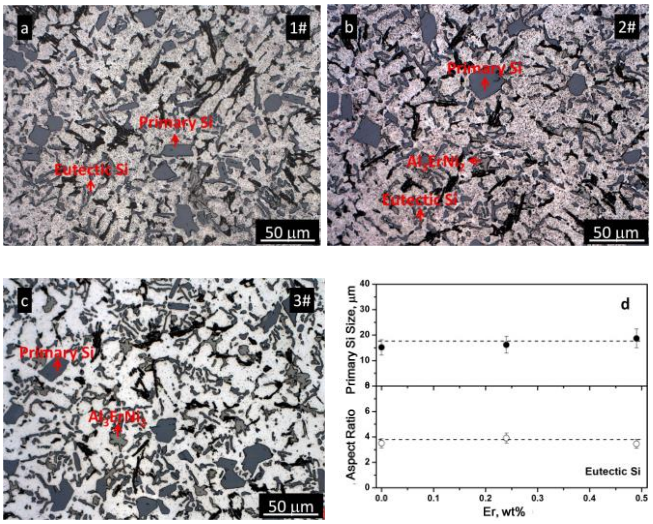


**Fig. 5.** The optical images of various additions of Er: a – 0 % Er; b – 0.24 % Er; c – 0.49 % Er in Al-Si alloys; d – the dependent of primary Si size and aspect ratio of eutectic Si on the Er additions at T6 state

For $Al_3(Er,Cu,Fe)(Ni, Si)_2$ phases, they have been kept stable during T6 heat treatments according to the XRD analysis (Fig. 2 b). In fact, their morphologies remain the star-like (Point 3) and irregular-shaped (Point 4) through the element mapping analysis (Fig. 6), and their sizes are still about 10 ~ 20 μm. The EDS analysis on this compound has further confirmed such stability, i.e., Al 47.72 at%, Si 21.34 at%, Ni 15.44 at%, Cu 4.08 at%, Fe 6.25 at% and Er 5.17 at% for the typical star-like compound (Point 3). Conclusively, this suggests the Er element is stably occupied by the $Al_3(Er,Cu,Fe)(Ni, Si)_2$ phase without any influence on the Si particles during the T6 process.

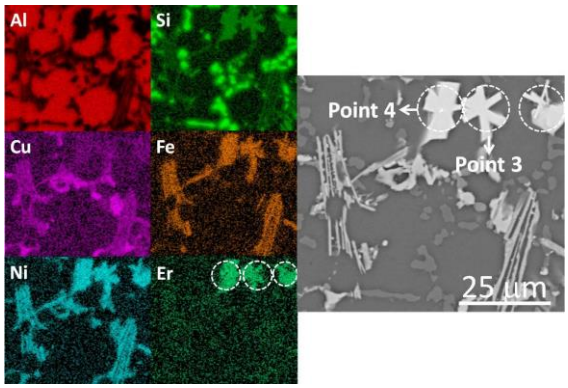


**Fig. 6.** Element mapping analysis of 0.49 wt.% Er added Al-Si alloy at T6 state

Fig. 7 a shows the correlations between ultimate tensile strengths (UTSs) / Fig. 7 b elongation at 350 °C and Er additions of Al-Si piston alloys. The UTSs of alloys at T5 state are found to reduce from 105 MPa to 94 MPa, and the elongation remains at ~ 7 % at 350 °C with the increasing Er content. At T6 state, the UTSs of alloys are progressively reduced from 96 MPa to 90 MPa at 350 °C as the Er additions elevate from 0 % to 0.49 %, and the elongation increases from 7.7 % to 9.6 %.

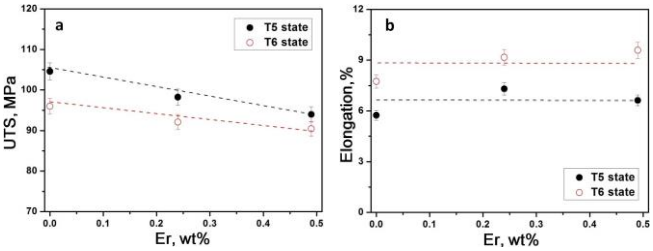


**Fig. 7.** The Er dependent behaviors: a – UTSs; b – elongation (%) in the Al-Si piston alloys at 350 °C

Generally, the UTSs have been decreased according to the growing Er addition for both states. In Al-Si piston alloys, Cu, Ni and Fe have been deemed as the main HT strengthening elements due to their abilities to create stable AlNiCu and AlFeSi compounds to sustain the HT loads. When Er is added into piston alloys, the $Al_3(Er,Cu,Fe)(Ni, Si)_2$ phase is steadily formed (Fig. 2, Fig. 4 and Fig. 6). In this compound, it contains ~ 5 at% Er, while the heat strengthening elements, including Cu, Ni and Fe, are much more consumed which is over 25 at% totally in the phase (Table 2).

**Table 2.** The composition of Er-containing compounds deriving from EDS analysis

| | Al, at% | Si, at% | Ni, at% | Cu, at% | Fe, at% | Er, at% | Suggested formula |
|---|---|---|---|---|---|---|---|
| T5 state (Fig. 4) | | | | | | | |
| Point 1 | 50.17 | 18.31 | 15.92 | 5.69 | 5.41 | 4.51 | $Al_3(Er, Cu, Fe) (Ni, Si)_2$ |
| Standard deviation | ± 1.51 | ± 0.55 | ± 0.48 | ± 0.17 | ± 0.16 | ± 0.14 | |
| Point 2 | 48.34 | 21.88 | 14.61 | 4.11 | 5.86 | 5.20 | $Al_3(Er, Cu, Fe) (Ni, Si)_2$ |
| Standard deviation | ± 1.45 | ± 0.66 | ± 0.44 | ± 0.12 | ± 0.18 | ± 0.16 | |
| T6 state (Fig. 6) | | | | | | | |
| Point 3 | 47.72 | 21.34 | 15.44 | 4.08 | 6.25 | 5.17 | $Al_3(Er, Cu, Fe) (Ni, Si)_2$ |
| Standard deviation | ± 1.43 | ± 0.64 | ± 0.46 | ± 0.12 | ± 0.19 | ± 0.16 | |
| Point 4 | 49.12 | 20.63 | 15.34 | 4.83 | 5.54 | 4.55 | $Al_3(Er, Cu, Fe) (Ni, Si)_2$ |
| Standard deviation | ± 1.47 | ± 0.62 | ± 0.46 | ± 0.14 | ± 0.17 | ± 0.14 | |

It is reasonable to infer that the HT stable intermetallics including these elements should be less created. The decreasing tendency in the UTS with the increasing Er content at T5 has proved this inference. Generally, the larger amount of Er added has led to a severer reduction in the HT strength. Treated by the T6 process on these materials, the reducing trend on HT strengths on the Er addition has not been changed, which is owing to highly stability of $Al_3(Er,Cu,Fe)(Ni, Si)_2$ phase.

In Fig. 7 a, the UTSs at T5 state can be notably higher over those at T6 state independent of Er additions in the same alloy. Based on the above analysis, in both heat treated Al-Si alloys, primary Si particles have the similar sizes. Nevertheless, the T6 treated alloys show the smaller sizes and aspect ratios of eutectic Si than those of T5 state.

Shown in the sixties by deep etching the Al matrix [48], the Al-Si alloy is identified as the three-dimensional (3D) connected eutectic Si structure embedded in the Al-matrix. Recently, Asghar et al.[49] has used X-ray tomography to reconstruct the 3D architecture of the Al-Si alloy, and characterized the alloy as a combination of an interconnected 3D structure of rigid eutectic Si and a ductile Al matrix. Generally, the 3D eutectic Si networks and primary aluminides are considered to work as major strengthening phases at HT [31, 32]. However, the solution treatment at HT has created spheroidized eutectic Si. As a result, the connectivity of eutectic Si network is lost, and the HT strengthening effect is degraded [31, 50, 51]. For example, Asghar et al. [50] investigated the morphology evolution of the Al-Si alloy using XRT. They found that the eutectic Si phases have transformed the morphologies from the highly interconnected lamellae into isolated rounded particles after exposure at 540 °C in the Al-12Si alloy. The HT strength of the Al-Si alloys was reduced in accompanying with the duration of solution treatment. Obeying the similar rules, the decreasing sizes and aspect ratios of eutectic Si particles through T6 process have caused the obvious reduction of tensile strength at 350 °C in the present study.

In addition, Asghar et al. [49 – 52] showed that the interconnectivity of eutectic Si was significantly reserved in the presence of Ni- and Fe- compounds. In association with the Si network, the Ni- and Fe- compounds can create a strongly interconnected 3D structure. The 3D structure has preserved its contiguity even experienced the solution treatment during T6. Even through, the HT strength at T6 was lower than the T5 Al-Si alloy. This finding is in good accordance with our experimental results. Since the interconnected eutectic Si structure has been kept, the T5 Al-Si alloys at have superior HT strengths to T6 state.

Nevertheless, the T6 state elongations are higher than at the T5 state (Fig. 7 b). At T5 state, the sharp edges of eutectic Si particles should act as stress concentrators. At T6 state, the eutectic Si particles are spheroidized through the HT process. These Si particles should be rounder in shape, which is benefited to ease the stress concentration. Therefore, the ductility of T6 Al-Si piston alloys should be higher over the T5 state.

## 4. CONCLUSIONS

The dependences of Er content (0 – 0.49 wt.%) on the microstructural evolution and related tensile strength at HT (350 °C) of the multicomponent Al-Si-Cu-Ni-Mg-Fe piston alloys were investigated. The microstructures and mechanical strengths at HT of the alloys were characterized and analyzed. It has listed the major conclusions thereby:

1. The identified compounds were similar in tested alloys at T5 and T6 heat treated states, including γ-$Al_3CuNi$, δ-$Al_7Cu_4Ni$, $Al_4Cu_2Mg_8Si_7$, and β-AlFeSi. The added Er element has led to the creation of the star-like and the irregular-shaped $Al_3(Er, Cu, Fe)(Ni, Si)_2$ phase.
2. The creation of $Al_3(Er, Cu, Fe)(Ni, Si)_2$ phase has consumed almost all the added Er element in the alloys, and the phase has stably existed in both T5 and T6 states. In this case, the chemical modification should not be effective on neither eutectic Si nor primary Si particles.
3. The UTSs of Al-Si alloys are reduced with the increasing Er addition, since the formation of $Al_3(Er, Cu, Fe)(Ni, Si)_2$ has used a larger amount of heat strengthening elements (i.e, Cu, Ni and Fe) at both states. The consumption can cause the less formed HT stable intermetallics. Furthermore, the aspect ratios are decreased for eutectic Si after the T6 treatment. In relation, the UTSs at 350 °C are also reduced. At HT, the eutectic Si networks should serve as the major strengthening phase. However, the solution treatment can impair the interconnected Si network, thus leading to reducing the strength at HT. On the other side, since the eutectic Si is spheroidized to ease the stress concentration, the ductility of the Al-Si alloy at T6 state should be improved over T5 state.


### *Acknowledgments*

The National Natural Science Foundation of China (Grant No. 51201099) and the Research Fund (Project No. 15X100040018) at Shanghai Jiao Tong University (P. R. China) are acknowledged to sponsor this work.


**REFERENCES**


1. **Ye, H.** An Overview of the Development of Al-Si-Alloy Based Material for Engine Applications *Journal of Materials Engineering and Performance* 12 (3) 2003: pp. 288 – 297. https://doi.org/10.1361/105994903770343132
2. **Miller, W.S., Zhuang, L., Bottema, J., Wittebrood, A.J., Smet, P.D., Haszler, A., Vieregge, A.** Recent Development in Aluminium Alloys for the Automotive Industry *Materials Science and Engineering: A* 280 (1) 2000: pp. 37 – 49. https://doi.org/10.1016/S0921-5093(99)00653-X
3. **Lai, H.Q., Fan, H.X., Xu, X.** Study and Application of Hypereutectic Al-Si Alloys *Automobile Technology & Material* 10 2001: pp. 21 – 24.
4. **Zhang, G., Li, B., Zhang, J., Feng, Z., Wei, Z., Cai, W.** Unique Cyclicd Deformation Behavior of A Heavily Alloyed Al-Si Piston Alloy at Different Temperatures *Progress in Natural Science: Materials International* 22 (5) 2012: pp. 445 – 451.

https://doi.org/10.1016/j.pnsc.2012.10.002

5. **Zhang, G., Zhang, J., Li, B., Cai, W.** Characterization of Tensile Fracture in Heavily Alloyed Al-Si Piston Alloy *Progress in Natural Science: Materials International* 21 (4) 2011: pp. 380 – 385. https://doi.org/10.1016/S1002-0071(12)60073-2
6. **Lee, J.A.** High-Strength Aluminum Casting Alloy for High-Temperature Applications (MSFC Center Director's Discretionary Fund Final Report, Project No. 97-10), 1998.
7. **Dahle, A.K., Nogita, K., McDonald, S.D., Dinnis, C., Lu, L.** Eutectic Modification and Microstructure Development in Al-Si Alloys *Materials Science and Engineering: A* 413 – 414 2005: pp. 243 – 248. https://doi.org/10.1016/j.msea.2005.09.055
8. **Abu-Dheir, N., Khraisheh, M., Saito, K., Male, A.** Silicon Morphology Modification in the Eutectic Al-Si Alloy Using Mechanical Mold Vibration *Materials Science and Engineering: A* 393(1 – 2) 2005: pp. 109 – 117. https://doi.org/10.1016/j.msea.2004.09.038
9. **Jiang, Q.C., Xu, C.L., Lu, M., Wang, H.Y.** Effect of New Al-P-Ti-TiC-Y Modifier on Primary Silicon in Hypereutectic Al-Si Alloys *Materials Letters* 59 (6) 2005: pp. 624 – 628. https://doi.org/10.1016/j.matlet.2004.10.042
10. **Chang, J., Moon, I., Choi, C.** Refinement of Cast Microstructure of Hypereutectic Al-Si Alloys Through the Addition of Rare Earth Metals *Journal of Materials Science* 33 (20) 1998: pp. 5015 – 5023. https://doi.org/10.1023/A:1004463125340
11. **Chen, Z.W., Jie, W.Q., Zhang, R.J.** Superheat Treatment of Al-7Si-0.55Mg Alloy Melt *Materials Letters* 59 (17) 2005: pp. 2183 – 2185. https://doi.org/10.1016/j.matlet.2004.08.047
12. **Matsuura, K., Kudoh, M., Kinoshita, H., Takahashi, H.** Precipitation of Si Particles in A Super-Rapidly Solidified Al-Si Hypereutectic Alloy *Materials Chemistry & Physics* 81 (2 – 3) 2003: pp. 393 – 395. https://doi.org/10.1016/S0254-0584(03)00030-0
13. **Srivastava, V.C., Mandal, R.K., Ojha, S.N.** Microstructure and Mechanical Properties of Al-Si Alloys Produced by Spray Forming Process *Materials Science and Engineering: A* 304 – 306 2001: pp. 555 – 558. https://doi.org/10.1016/S0254-0584(03)00030-0
14. **Abramov, V.O., Abramov, O.V., Straumal, B.B., Gust, W.** Hypereutectic Al-Si Based Alloys with A Thixotropic Microstructure Produced by Ultrasonic Treatment *Materials & Design* 18 (4 – 6) 1997: pp. 323 – 326. https://doi.org/10.1016/S0261-3069(97)00072-1
15. **Jiang, W., Fan, Z., Dai, Y., Li, C.** Effects of Rare Earth Elements Addition on Microstructures, Tensile Properties and Fractography of A357 Alloy *Materials Science and Engineering: A* 597 2014: pp. 237 – 244. https://doi.org/10.1016/j.msea.2014.01.009
16. **Li, Q., Xia, T., Lan, Y., Zhao, W., Fan, L., Li, P.** Effect of Rare Earth Cerium Addition on the Microstructure and Tensile Properties of Hypereutectic Al-20%Si Alloy *Journal of Alloys & Compounds* 562 2013: pp 25 – 32. https://doi.org/10.1016/j.jallcom.2013.02.016
17. **Nogita, K., Yasuda, H., Yoshiya, M., McDonald, S.D., Uesugi, K., Takeuchi, A., Suzuki, Y.** The Role of Trace Element Segregation in the Eutectic Modification of Hypoeutectic Al-Si Alloys *Journal of Alloys & Compounds* 489 (2) 2010: pp. 415 – 420. https://doi.org/10.1016/j.jallcom.2009.09.138
18. **Han, N., Bian, X., Yin, K., Yao, X.** Modification Effect of Er on Hypoeutectic Al-8Si Alloy *Journal of Rare Earths* 23 (S1) 2005: pp. 474 – 477.
19. **Xing, P., Gao, B., Zhuang, Y., Liu, K., Tu, G.** Effect of Erbium on Properties and Microstructure of Al-Si Eutectic Alloy *Journal of Rare Earths* 28 (6) 2010: pp. 927 – 930. https://doi.org/10.1016/S1002-0721(09)60222-2
20. **Xing, P., Gao, B., Zhuang, Y., Liu, K., Tu, G.** On the Modiffcation of Hypereutectic Al-Si Alloys Using Rare Earth Er *Acta Metallurgica Sinica* 23 (5) 2010: pp. 327 – 333. https://doi.org/10.11890/1006-7191-105-327
21. **Hu, X., Jiang, F., Ai, F., Yan, H.** Effects of Rare Earth Er Additions on Microstructure Development and Mechanical Properties of Die-Cast ADC12 Aluminum Alloy *Journal of Alloys & Compounds* 538 2012: pp. 21 – 27. https://doi.org/10.1016/j.jallcom.2012.05.089
22. **Li, Q., Xia, T., Lan, Y., Zhao, W., Fan, L.** Effects of Rare Earth Er Addition on Microstructure and Mechanical Properties of Hypereutectic Al-20% Si Alloy *Materials Science and Engineering: A* 588 2013: pp. 97 – 102. https://doi.org/10.1016/j.msea.2013.09.017
23. **Shi, Z.M., Wang, Q., Zhao, G., Zhang, R.Y.** Effects of Erbium Modification on the Microstructure and Mechanical Properties of A356 Aluminum Alloys *Materials Science and Engineering: A* 626 2015: pp. 102 – 107. https://doi.org/10.1016/j.msea.2014.12.062
24. **Tsai, Y.C., Chou, C.Y., Lee, S.L., Lin, C.K., Lin, J.C., Lim, S.W.** Effect of Trace La Addition on the Microstructures and Mechanical Properties of A356 (Al-7Si-0.35Mg) Aluminum Alloys *Journal of Alloys & Compounds* 487 2009: pp. 157 – 162. https://doi.org/10.1016/j.msea.2014.12.062
25. **Yi, H., Zhang, D.** Morphologies of Si Phase and La-Rich Phase in As-Cast Hypereutectic Al-Si-xLa Alloys *Materials Letters* 57 2003: pp. 2523 – 2529. https://doi.org/10.1016/S0167-577X(02)01305-8
26. **Patakham, U., Kajornchaiyakul, J., Limmaneevichitr, C.** Grain Refinement Mechanism in An Al-Si-Mg Alloy with Scandium *Journal of Alloys & Compounds* 542 2012: pp. 177 – 186. https://doi.org/10.1016/j.jallcom.2012.07.018
27. **Zhang, W., Liu, Y., Yang, J., Dang, J., Xu, H., Du, Z.** Effects of Sc Content on the Microstructure of As-Cast Al-7 wt% Si Alloys *Materilas Characterization* 66 2012: pp. 104 – 110. https://doi.org/10.1016/j.matchar.2011.11.005
28. **Yu, S., Jin, Y., Xiong, W., Liu, Y.** Study on Microstructure and Mechanical Properties of ZL107 alloy Added with Yttrium *Journal of Rare Earths* 31 (2) 2013: pp. 198 – 203. https://doi.org/10.1016/S1002-0721(12)60258-0
29. **Li, B., Wang, H., Jie, J., Wei, Z.** Microstructure Evolution and Modification Mechanism of the Ytterbium Modified Al-7.5%Si-0.45%Mg Alloys *Journal of Alloys & Compounds* 509 2011: pp. 3387 – 3392. https://doi.org/10.1016/j.jallcom.2010.12.081
30. **Belov, N., Eskin, D., Aksenov, A.** Multicomponent Phase Diagrams: Applications for Commercial Aluminum Alloys, Elsevier, Oxford, 2005.
31. **Requena, G. Degischer, H.P.** Three-Dimensional Architecture of Engineering Multiphase Metals *Annual Review of Materials Research* 42 2012: pp. 145 – 161. https://doi.org/10.1146/annurev-matsci-070511-155109

32. **Requena, G., Garces, G., Asghar, Z., Marks, E., Staron, P., Cloetens, P.** The Effect of the Connectivity of Rigid Phases on Strength of Al-Si Alloys *Advanced Engineering Materials* 12 (8) 2011: pp. 674 – 684. https://doi.org/10.1002/adem.201000292

33. **Li, Y., Yang, Y., Wu, Y., Wang, L., Liu, X.** Supportive Strengthening Role of Cr-rich Phase on Al-Si Multicomponent Piston Alloy at Elevated Temperature *Materials Science and Engineering: A* 528 2011: pp. 4427 – 4430. https://doi.org/10.1016/j.msea.2011.02.047

34. **Li, Y., Yang, Y., Wu, Y., Wang, L., Liu, X.** Quantitative Comparison of Three Ni-containing Phases to the Elevated-Temperature Properties of Al-Si Piston Alloys *Materials Science and Engineering: A* 527 2010: pp. 7132 – 7137. https://doi.org/10.1016/j.msea.2010.07.073

35. **Stadler, F., Antrekowitsch, H., Fragner, W., Kaufmann, H., Uggowitzer, P.J.** The Effect of Ni on the High-Temperature Strength of Al-Si Cast Alloys *Materials Science Forum* 690 2011: pp. 274 – 277. https://doi.org/10.4028/www.scientific.net/MSF.690.274

36. **Sui, Y., Wang, Q., Liu, T., Ye, B., Jiang, H., Ding, W.** Influence of Gd Content on Microstructure and Mechanical Properties of Cast Al-12Si-4Cu-2Ni-0.8Mg alloys *Journal of Alloys & Compounds* 644 2015: pp. 228 – 235. https://doi.org/10.1016/j.jallcom.2015.04.164

37. **Gao, T., Zhu, X., Sun, Q., Liu, X.** Morphological Evolution of ZrAlSi Phase and Its Impact on the Elevated-Temperature Properties of Al-Si Piston Alloy *Journal of Alloys & Compounds* 567 2013: pp. 82 – 88. https://doi.org/10.1016/j.jallcom.2013.03.064

38. **Hu, P., Su, Y., Chen, W., Jiang, Y.** Effects of Ce, Mn, Cr on the Microstructure and Properties of High-iron Eutectic Al-Si Piston Alloy *Advanced Materials Research* 652 – 654 2013: pp. 1023 – 1029. https://doi.org/10.4028/www.scientific.net/AMR.652-654.1023

39. **Zhou, L., Peng, Y., Zhu, X., Zhang, G., Yang, L., Shi, H.** Influence of Ti to the Microstructure and Mechanical Properties of Al-12Si-3.2Cu-1Mg-2.4Ni Piston Alloy *Applied Mechnics & Materials* 477 – 478 2014: pp. 1278 – 1283. https://doi.org/10.4028/www.scientific.net/AMM.477-478.1278

40. **Yang, Y., Yu, K., Li, Y., Zhao, D., Liu, X.** Evolution of Nickel-Rich Phases in Al-Si-Cu-Ni-Mg Piston Alloys with Different Cu Additions *Materials & Design* 33 2012: pp. 220 – 225. https://doi.org/10.1016/j.matdes.2011.06.058

41. **Yang, Y., Zhong, S.Y., Chen, Z., Wang, M., Ma, N., Wang, H.** Effect of Cr Content and Heat-treatment on the High Temperature Strength of Eutectic Al-Si Alloys *Journal of Alloys & Compounds* 647 2015: pp. 63 – 69. https://doi.org/10.1016/j.jallcom.2015.05.167

42. **Tsai, Y.C., Lee, S.L., Lin, C.K.** Effect of Trace Ce Addition on the Microstructures and Mechanical Properties of A356 (Al-7Si-0.35Mg) Aluminum Alloys *Journal of the Chinese Institute of Engineers* 34 (5) 2011: pp. 609 – 616. https://doi.org/10.1080/02533839.2011.577598

43. **Manasijevic, S., Radisa, R., Markovic, S., Acimovic-Pavlovic, Z., Raic, K.** Thermal Analysis and Microscopic Characterization of the Piston Alloy AlSi13Cu4Ni2Mg *Intermetallics* 19 2011: pp. 486 – 492. https://doi.org/10.1016/j.intermet.2010.11.011

44. **Martin, J.W., Doherty, R.D., Cantor, B.** Stability of Microstructure in Metallic Systems, Cambridge University Press, 1997.

45. **Ogris, E., Wahlen, A., Lüchinger, H., Uggowitzer, P.J.** On the Silicon Spheroidization in Al-Si Slloys *Journal of Light Metals* 2 (4) 2002: pp. 263 – 269. https://doi.org/10.1016/S1471-5317(03)00010-5

46. **Sebaie, O.E., Samuel, A.M., Samuel, F.H., Doty, H.W.** The Effects of Mischmetal, Cooling Rate and Heat Treatment on the Eutectic Si Particle Characteristics of A319.1, A356.2 and A413.1 Al-Si Casting Alloys *Materials Science and Engineering: A* 480 (1 – 2) 2008: pp. 342 – 355. https://doi.org/10.1016/j.msea.2007.07.039

47. **Fernández-Gutiérrez, R. Requena, G.C.** The Effect of Spheroidisation Heat Treatment on the Creep Resistance of a Cast AlSi12CuMgNi Piston Alloy *Materials Science and Engineering: A* 598 2014: pp. 147 – 153. https://doi.org/10.1016/j.msea.2013.12.093

48. **Asghar, Z., Requena, G., Boller, E.** Three-Dimensional Rigid Multiphase Networks Providing High-temperature Strength to Cast AlSi10Cu5Ni1-2 Piston Alloys *Acta Materialia* 59 2011: pp. 6420 – 6432. https://doi.org/10.1016/j.actamat.2011.07.006

49. **Bell, J.A.E., Winegard, W.C.** Interconnexion of Silicon in Modified Aluminium-Silicon Eutectic *Nature* 208 1965: pp. 177. https://doi.org/10.1038/208177a0

50. **Asghar, Z., Requena, G., Kubel, F.** The Role of Ni and Fe Aluminides on the Elevated Temperature Strength of An AlSi12 Alloy *Materials Science and Engineering:A* 527 2010: pp. 5691 – 5698. https://doi.org/10.1016/j.msea.2010.05.033

51. **Asghar, Z., Requena, G.** Three Dimensional Post-Mortem Study of Damage after Compression of Cast Al-Si Alloys *Materials Science and Engineering: A* 591 2014: pp. 136 – 143. https://doi.org/10.1016/j.msea.2013.10.067

52. **Asghar, Z., Requena, G., Degischer, H.P., Cloetens, P.** Three-Dimensional Study of Ni Aluminides in An AlSi12 Alloy by Means of Light Optical and Synchrotron Microtomography *Acta Materialia* 57 2009: pp. 4125 – 4132. https://doi.org/10.1016/j.actamat.2009.05.010